RESEARCH ARTICLE

Experimental study on the characteristics of train-induced vibration in a new structure of metro depot

Yanming Chen [1] · Qingsong Feng [1] · Qinjie Liu [1] · Jian Jiang [1]

Abstract

In order to improve the utilization rate of expensive and very limited urban land, a new structure system, underground metro depot, has been developed and applied in several cities in China. The underground metro depot, which is built underground, can be multiple stories, and allows other developments on top, has become increasingly popular in recent years. Since there are other developments on top, the vibration induced by the trains frequently entering and exiting the depot cannot be ignored. To better understand the characteristics of the train-induced vibration in the underground metro depot, a series of field tests were conducted on a two-story underground depot which is the largest underground metro depot in Asia. The results show that the main frequency components of vibration source are between 50 and 200 Hz and the level of that in the first floor underground is larger than that in the second floor underground due to the train floor structure interaction when the train running on the first floor underground. The vibration in the top platform decreases linearly with the distance from the measuring point to the center line of the track. When the train is running on the track at the edge area, the linear attenuation rate was about 0.2dB/m. It is easy to excite the vibration mode of the floor structure when the train is running on the first floor underground, so the vibration in the top platform induced by the train running on the first floor underground was much larger than the train running on the second floor underground. In the future design, if the underground depot has more than one floor, the structural dynamic behavior of over-track buildings induced by the train running on the floor slab underground should be the focus. The throat area has many rail joints and turnouts which can lead to a larger vibration level, the level easy to exceed the limit given for human vibration comfort. If developments are proposed on top of the throat area, the vibration level should be carefully checked in the area within 30 m from the track to avoid potential later vibration problem.

Keywords Underground metro depot · Over-track building · Train-induced vibration · Field measurement · Vibration transmission · Vibration comfort level evaluation'

Introduction

Urban traffic congestion has become increasingly serious in many Chinese cities due to the very high urbanization speed and the continuous growth of urban population in the past decades. To resolve this problem, the development of public transportation, especially metro, has been moved to the top agenda of many local government's infrastructure

development strategy. Compared with many other transport systems, metro is relatively more reliable and efficient. It also has the advantages of high-speed, large transport volume, and high comfort level. It can link the major areas in the city and ease the pressure for other public transport systems. A lot of developments have been carried out very rapidly in recent years. By the end of December 2020, 45 cities in mainland China had opened urban rail transit lines with a total mileage of 7978.19 km (China Association of Metros 2021), ranked the first in the world. Metro depot, the structure where the metro trains are parked, inspected, and repaired, have also been built as part of the development. Since the metro depot requires a large amount of space, it's not land efficient in the urban area. To improve the utilization rate of the expensive and very limited urban land, further developments such as residential and commercial buildings, often called over-track

✉ Qingsong Feng
   1439670627@qq.com

[1] School of Civil Engineering and Architecture, East China Jiaotong University, Nanchang 330013, Jiangxi, China

buildings, can be built on top of the metro depot platform. Up to now, more than 27 cities in mainland China have developed this type of structure of metro depot with the over-track buildings on top. However, at present, most of these metro depots are built on the ground-level. Compared with these ground-level depots, the underground depots (see Fig. 1), which transfer the working area from the ground to the underground, are more expensive to build but have an even better land utilization rate. The underground depot has received many interests in recent years, especially in large cities where the land is extremely expensive.

Although the underground metro depot has many advantages, the vibration and noise induced by the trains entering and exiting the depot can potentially be a huge problem. The vibration induced by train is rarely strong enough to cause safety concerns of the building structure, but it can reach a level affecting the comfort of human and limit the usage of the building constructed on top of the depot. The associated noise induced by structural vibration has very low frequencies (Aires et al. 2017). Long-term explosion in such environment can gradually cause damage to the hearing as well as further psychological problems. There are some researches that have been done for ground-level metro depots (Zou et al. 2015; Tao et al. 2019a). These studies have found that, in some cases, the vibration or noise levels in the over-track buildings have exceeded the limits given by the US Federal Transit Administration (FTA) (Federal Transit Administration 2006) and China State Bureau of Environment Protection (China's State Environmental Protection Administration 1988). Compared with the ground-level depot, the vibration and noise problems in the underground metro depot can be more serious. The underground depot normally has multiple stories underground with tracks built in each floor. Unlike in the ground-level depot, the vibration is mainly transmitted to the upper-level platform and buildings through columns and building structures when the train is running on the first floor underground, with none or very limited attenuation from the soil (see Fig. 2).

Within the underground metro depot, the vibration characteristics in the throat area and the inspection area are especially important. The throat area links the entrance/exit area and the

inspection area. There are many rail joints, turnouts, and curves with small radius in this area, as the number of tracks changes from several to several dozens in this area. The inspection area is the place where the trains are parked and checked daily. It occupies the largest area in the depot and often has residential buildings on the top platform. A better understanding of the vibration characteristics, including the vibration source, vibration transmission characteristics, and the influence on comfort level in these area, can help to identify and resolve current vibration problem occurring in such type of structure of metro depot. It can also provide valuable information and data to assist the planning and development of new underground metro depots in the future.

With the continuous improvement of people's requirements for living environment, more and more attention has been paid to the vibration and noise problems induced by train pass-by events. In the past, there have been many studies on the vibration of buildings around railways or above tunnels, including the vibration characteristics of buildings (Persson and Persson 2016; Sanayei et al. 2013, 2014; Kouroussis et al. 2011a, b, 2013, 2015), vibration transmission and reduction measures (Metrikine and Vrouwenvelder 2000; Vogiatzis and Mouzakis 2018; Ju 2007; Connolly et al. 2014; Galvín and Domínguez 2009; He et al. 2020), and vibration prediction method (López-Mendoza and Romero 2017; Lopes and Costa 2014; Hussein and Hunt 2015; Coulier et al. 2014; Ma et al. 2020). With the increasing tension of urban land utilization rate, a new structure of metro depot with over-track buildings gradually comes into people's view. At the same time, the vibration of the over-track buildings induced by the train entering and leaving the depot has also attracted many scholars' attention and research. Tao et al. (2019a, b); Zou et al. (2015, 2017, 2018, 2020) carried out field measurement and theoretical analysis on underground metro depot at Guangzhou and Shenzhen of China, respectively, and they predicted the vibration induced by trains and analyzed the transmission characteristics of the vibration in these metro depot. Cao and Guo (2018) measured and theoretically analyzed the residential building over the metro depot. He pointed out that the distance between the railway track and measure points had an obvious influence on vibration response. When

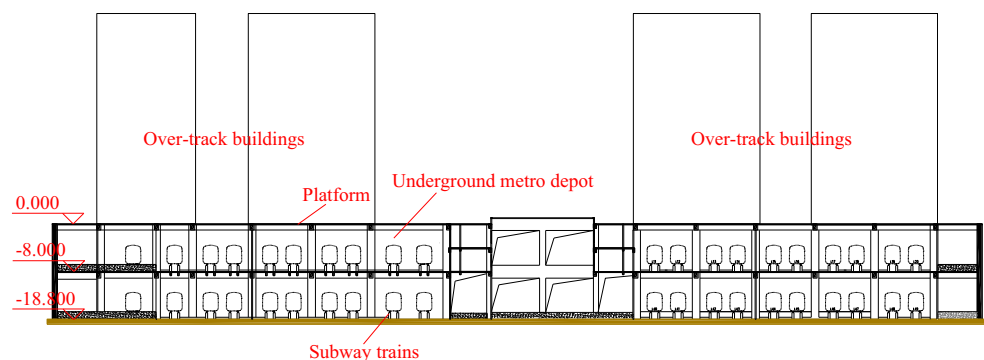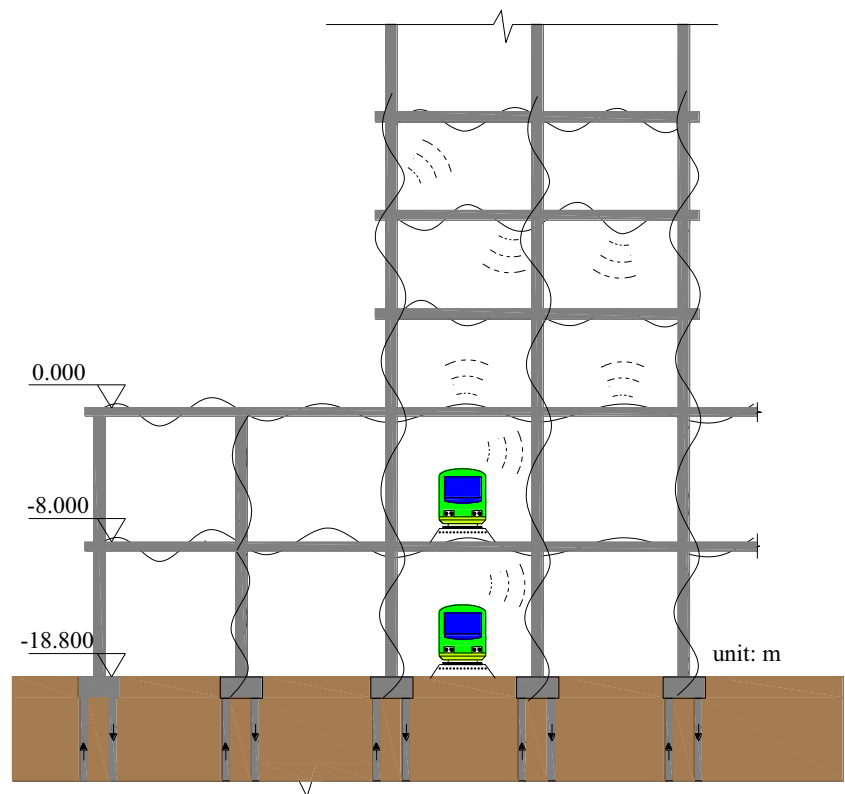Fig. 1 Underground two-story metro depot and over-track buildings

Fig. 2 The diagram of vibration transmission in the two-story metro depot

the distance between the building and the railway track is more than 12 m, the vibration level meets the requirement. Although the train speed is only 5 km/h, the vibration level of the bottom two floors of the over-track building still exceeded the limit value when the subway train runs in/out of the metro depot. Guo et al. (2017) studied the influence of train speed and fastener configuration on the vibration response of buildings in a 3-story metro depot through numerical simulation. Xie et al. (2013) summarized the general process of the vibration comfort level analysis on the over-track buildings through field measurement and theoretical analysis and proposed the refined finite element model based on the human comfort evaluation. In addition, the vibration and noise problems of the over-track buildings induced by bridge cranes in the maintenance and repair shed of metro depot should not be ignored, as the bridge crane-induced vibration was comparable to the levels of train-induced vibration (He 2018, 2019).

All the previous studies mentioned above focused on the metro train-induced vibration in the nearby buildings or ground-level metro depot, where the vibration must transmit through soil to the structure and can be significantly attenuated by the soil. Compared with these buildings, the underground metro depot with multiple stories has the vibration transmitted path via concrete column to the upper buildings directly without soil attenuation; therefore, the vibration characteristics may be very different. This paper carried out an experimental study to obtain the first hand field measurement data from the

largest underground metro depot in Asia, in order to better understand the characteristics of train-induced vibration in the underground multiple-story metro depot. The experimental setup is introduced in the next section. Results are carefully analyzed in third section, and conclusions are given in the last section.

Experiment setup

Testing site

The underground metro depot studied in this paper is located in Chengdu, a major city in the western region of China, with a population of 16.33 million. By the end of 2020, the total length of Chengdu Metro line was 558 km. According to the fourth phase plan of Chengdu Metro (2019–2024) (National Development and Reform Commission of China 2019), by the end of the 2024, the operation mileage of Chengdu Metro line will reach 714 km.

The size of the planned over-track buildings on top of this depot is 495 m in the north–south direction and 183 m in the east–west direction, with a total floor area of 177,000 m². This depot is one of the most important parts of the metro train base, as all the trains used in the Chengdu Metro Line 7 are parked and inspected here. The main structure of the depot is an underground two-story–reinforced concrete frame with

large base and multiple-tower structures. The foundation type below the metro depot is pile foundation. The soil on the site consists of multiple layers, from bottom to top, inducing miscellaneous fill, silty clay, sandy soil, and Pleistocene soft rock, and the soil dynamic parameters are shown in Table 1.

The depot has four main areas, link line area, operation area, throat area, and inspection area, named as A/B/C/D areas, respectively. The depot can park 76 subway trains at the same time (38 parking spaces in each underground floor).

The planning permission has been granted to construct a number of multiple-story residential and commercial buildings on top of the metro depot, as well as the metro operation control center and the metro parking garage. The planning renderings is shown in Fig. 3. Section layout is shown in Fig. 4.

The test sections were placed in the throat area (section C) and inspection area (section D) in the depot. Photos of these two sections are shown in Fig. 5. The basic information of the train and the track in the metro depot is shown in Table 2.

Measurement points arrangement and testing equipment

When the train is running on the multistory depot structure, wheel–rail interaction will excite the vibration of the rail and other track structures. Then the vibration will transmit along structure components such as floor slab and column to the buildings above the depot. In this paper, the vibration of track structures is considered as the vibration source. In order to study the characteristics of the vibration source in the depot, the vibration source measurement points were set on the rail (C8 and C10) and track-bed (C9 and C11) on the first and second underground floor, respectively, at the throat area. In the inspection area, the track is supported by short columns, and the inspection pit is under the track, so the vibration source measurement points were set on the rail (D6 and D9) and the supporting column (D7 and D10) . To investigate the transmission characteristics of vibration between floors, measurement points were also set in the center of each floor (D8 and D11) at the inspection area. The layout of measuring points is shown in Fig. 6. The thickness of the floor slab is 200 mm, and the column size is 800 × 800 mm in Fig. 6.

To study the transmission characteristics of vibration inside the top platform, acceleration sensors were set in the platform directly on top of the metro depot. The measurement points were located in the middle of each floor span, in a line perpendicular to the track direction, as shown in Fig. 7. Photos of the setting on the site are shown in Figs. 8 and 9.

DATaRec4 DIC24 data acquisition instrument (Fig. 10) from the German HEAD Acoustics GmbH, ICP, and 941B vibration sensors was used in the test. All the equipment and sensors were calibrated before the test. The vibration signal was continuously monitored during the test, and the acquisition was trigger for a 30-s recording by each train pass-by event.

Results and discussion

Vibration source characteristics

Table 3 shows the vibration source response obtained at the throat area and the inspection area. Figures 11 and 12 illustrate the acceleration time history and power spectrum density (PSD) of the vibration source.

As shown in Table 3 and Fig. 11, in the throat area, the average acceleration peak value obtained on the rail in the first floor underground (12.78 m/s^2) is smaller than that in the second floor underground (17.67 m/s^2), while the average acceleration peak value obtained on the ballast bed of the first floor underground (0.51m/s^2) is larger than that in the second floor underground (0.26 m/s^2). The average train speed in the second floor underground was about 20.2 km/h, and it was about 14.4 km/h in the first floor underground. Considering the other conditions are roughly the same in these two floors, the train speed is the main reason causing the difference of the rail average peak acceleration between these two floors. The vibration response of the ballast bed is influenced by many factors, including the type of rail fastener, train type, train load, train speed, and support conditions of the ballast bed. The train type, load, and rail fastener in these two floors are very much the same. The ballast bed in the first floor underground is placed on the floor which is supported by columns, and the ballast bed in the second floor underground is directly on top of the foundation in the ground. The bracing stiffness of

Table 1 Soil dynamic parameters	Soil layer	Thickness (m)	Density (kg/m^3)	Shear wave velocity (m/s)	Poisson's ratio	Elastic modulus (MPa)
	Miscellaneous fill	16	1850	150.7	0.38	116
	Silty clay	8	1950	189.9	0.38	194
	Sandy soil	8	1980	201.5	0.35	217
	Pleistocene soft rock	33	2310	800	0.30	3907

Fig. 3 Renderings of the over-track buildings on top of the metro depot. **a** Full view, **b** cross-section profile

the ballast bed in the first floor underground is much less than that in the second floor underground. The vibration energy in the second floor underground can also be partially attenuated by the surrounding soil. Therefore, the attenuation of vibration energy from the rail to the ballast bed is larger in the second floor underground than the first floor underground. As a result, although the train speed in the second floor underground is faster, the vibration response on the ballast bed is still smaller than the first floor underground.

In the inspection garage, the average peak value of the vibration acceleration obtained on the rail and supporting column are 12.73 and 0.61 m/s^2, respectively, in the first floor underground and 2.68 and 0.16 m/s^2, respectively, in the second floor underground. The values in the first floor underground are 4.8 and 3.8 times larger than those in the second floor underground. This may be due to the fact that the supporting columns sit on top of the floor structure in the first

floor underground but directly on top of the foundation in the second floor underground. The local bending vibration of the floor structure can be stimulated by the running trains and increases the vibration on the supporting column in the first floor underground. In addition, the first floor underground uses ordinary rail, while the second floor underground uses damping rail. The damping rail can absorb part of the vibration energy through the damping material. Therefore, the rail's vibration response in the second floor underground is smaller than that in the first floor underground.

In Fig. 12, in frequency domain, the rail has a wider vibration frequency band than the ballast bed, with the main energy below 900 Hz and distributed fairly even. Compared with the rail, the ballast bed and supporting column have more concentrated vibration energy in the frequency bands from 50 to 200 Hz. This indicated that the vibration energy above 200 Hz was attenuated rapidly when transmitted from the rail to the ballast
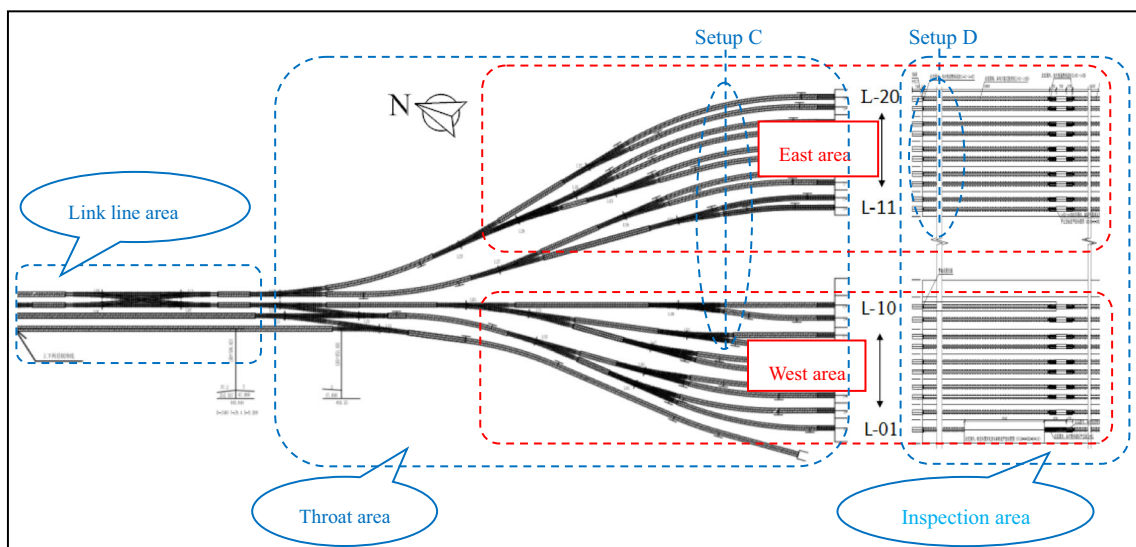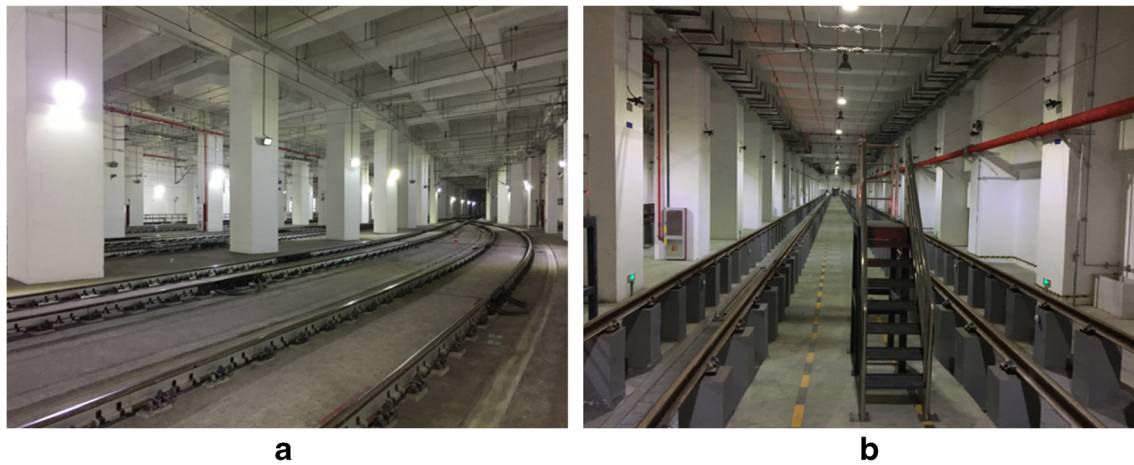

Fig. 4 Plan view of metro depot

Fig. 5 Rail types in metro depot. **a** Throat area track and **b** inspection area track

bed and the supporting column. As we know, the frequency distribution of vibration in buildings is related to the vibration source characteristics. Therefore, the natural frequency of the over-track building floor slab should avoid the main frequency range of the vibration source.

Figure 13 shows the rail and ballast bed acceleration levels in the throat area in 1/3 octave bands. From the data shown in Fig. 1 except the frequency bands from 31.5 to 63Hz, the vibration acceleration level of the rail in the second floor underground is larger than that in the first floor underground. The vibration acceleration level of ballast bed in the first floor underground is larger than that in the second floor underground in all frequency bands. This agreed with the results obtained in time domain as seen in Fig. 11. The spectrum of ballast bed in 1/3 octave bands shows similar trend in both floors, with major peak occurring at about 100 Hz.

The rail-ballast vibration attenuation in the throat area was further analyzed by using the insertion loss ratio. The insertion loss ratio is defined as

$$\eta_i = \frac{VLR_i - VLB_i}{VLR_i} \tag{1}$$

where:

η_i is the rail-ballast insertion loss ratio at each frequency band, dimensionless

VLR_i is the vibration acceleration level of rail at the ith 1/3 octave frequency band, dB

VLB_i is the vibration acceleration level of ballast bed at the ith 1/3 octave frequency band, dB。

Figure 14 shows the rail-ballast bed insertion loss ratio in the throat area. From the figure, the insertion loss ratio in the second floor underground is much larger than that in the first floor underground, indicating the vibration attenuation from the rail to ballast bed is larger in the second floor underground. The maximum insertion loss ratio in the second floor underground is 0.7, and it is 0.45 in the first floor underground. This also explains why the vibration response of the rail is larger in the second floor underground, but the vibration response of ballast bed is larger in the first floor underground.

## Vibration transmission characteristics

In order to study the vibration transmission characteristics inside the underground metro depot, experiment data from typical train pass-by events were selected to conduct transmission analysis.

Table 2 The basic information of train track in depot

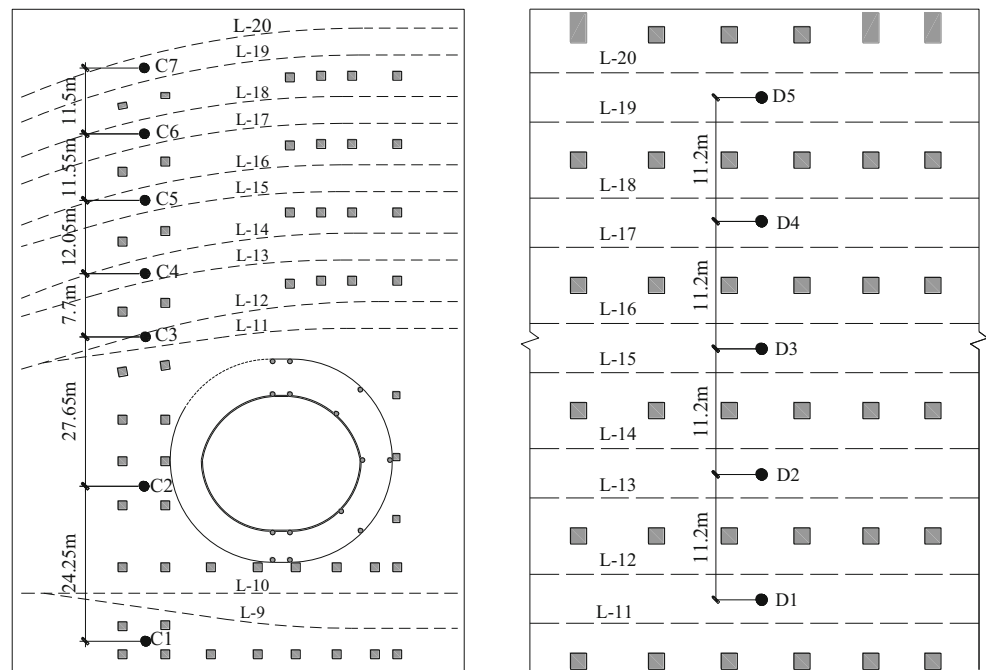| Test area	Throat area	Inspection area
Train parameters	Type A, 23 m in length, 3.1 m in width, and 16 t in axle load	
Track condition	50 kg/m damped rail	First floor underground: 50 kg/m ordinary seamless rail Second floor underground: 50 kg/m damped rail
Fastener	CZI fastener	Double-layer nonlinear damping fastener
Rail support	Short sleeper	Column type support
Loading condition	Empty train	
Train speed	First floor underground: 14.4 km/h Second floor underground: 20.2 km/h	First floor underground: 9.9 km/h Second floor underground: 14.2 km/h
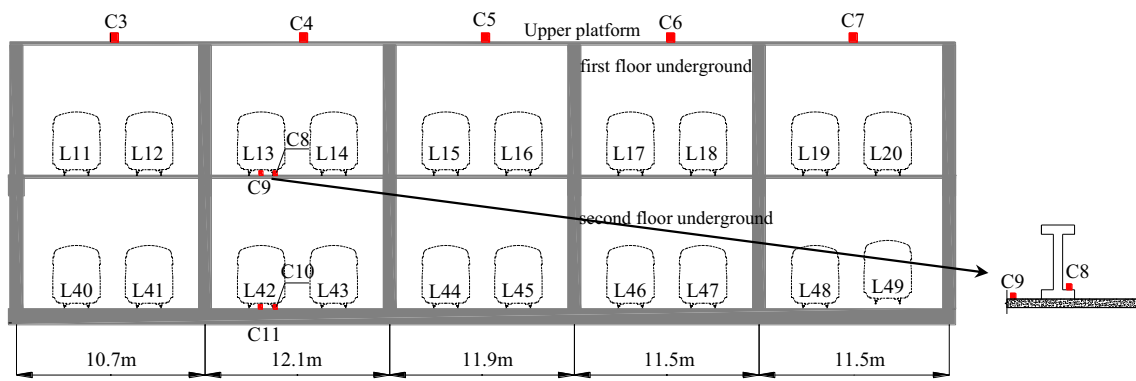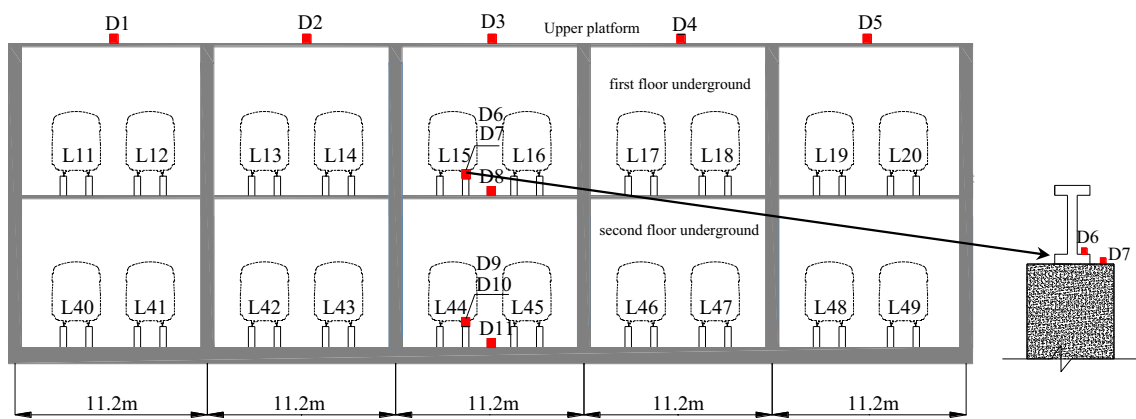
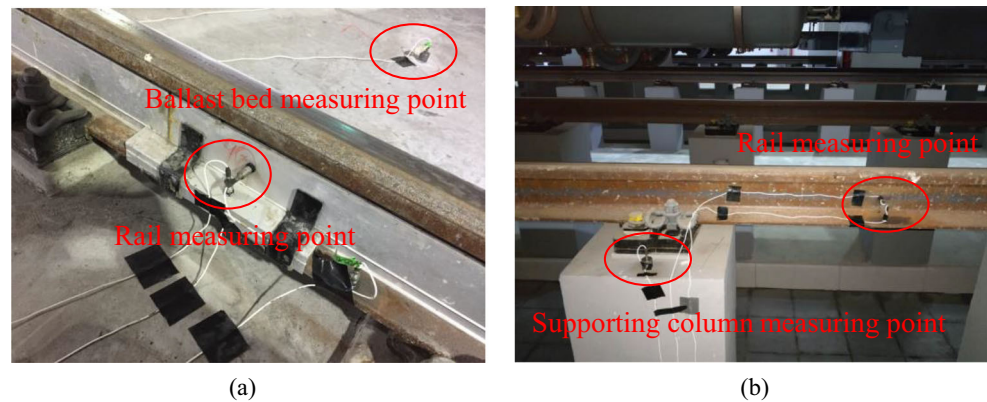**Fig. 6** Vertical plan of measurement locations in the metro depot. **a** Throat area and **b** inspection area

Fig. 7 Plane view of measurement locations on the platform of metro depot. **a** Throat area and **b** inspection area

Fig. 8 Sensor setups of vibration source in the metro depot. **a** Throat area and **b** inspection area

(a)

(b)

Vibration transmission along the top platform

Several measurement data were conducted to investigate how the vibration propagates along the top platform, when trains were running in the throat area and the inspection area below, including:

Measurement setting 1: The train was passing by side track and directly below C7 at the throat area on the first floor underground.

Measurement setting 2: The train was passing by the middle track directly below C4 at the throat area on the first floor underground.

Measurement setting 3: The train was passing by side track directly below D5 at the inspection area on the first floor underground.

Measurement setting 4: The train was passing by the middle track directly below D3 at the inspection area on the first floor underground.

Fig. 9 Sensor setups on the platform

(1) **Vibration level analysis**

Figure 15 shows the average acceleration level with error bar under different settings. Regression analysis was conducted between the horizontal distance of the measuring point to the center line of the running track and the average vibration level, to obtain the regression curves and fitting formulas which were also shown in the figures.

As shown in Fig. 15, when the train was passing by the side track at the throat area (setting 1), the vibration level measured in the top platform decreases with distance linearly with a speed of about 0.2d B/m. In the current plan, commercial and residential buildings will be constructed on top of this area. The acceleration level measured in the platform directly on top of the train is about 78 dB. It is already 6 dB larger than the night threshold, 72 dB for such buildings, given by the standard of vibration in urban area environment (GB 10070-1988) in China. Therefore, the vibration level within 30 m from the track should be monitored, and mitigation measures may need to be considered, if the current plan goes ahead without any change.

When the train was passing by the middle track at the throat area (setting 2), the vibration level measured in the top platform decreases with distance linearly in both directions, with the speed of 0.1 and 0.2 dB/m respectively. When the vibration reached the measuring point C7 which is about 35.1 m from the center of the track and inside the end floor panel, the vibration level increased. This may be due to the fact that the level obtained was influenced by the superposition of reflected waves.

When the train was passing by the side track at the inspection area (setting 3), the vibration level measured in the top platform decreases with distance linearly with a speed of about 0.2 dB/m and a linear fitting deterministic coefficient of $R^2 = 0.98$. When the train was passing by the middle track at the inspection area (setting 4), the vibration level measured in the top platform decreases with distance linearly in both directions, with a speed of about 0.1 dB/m. The linear fitting

Fig. 10 DATaRec 4 DIC24 data acquisition instrument
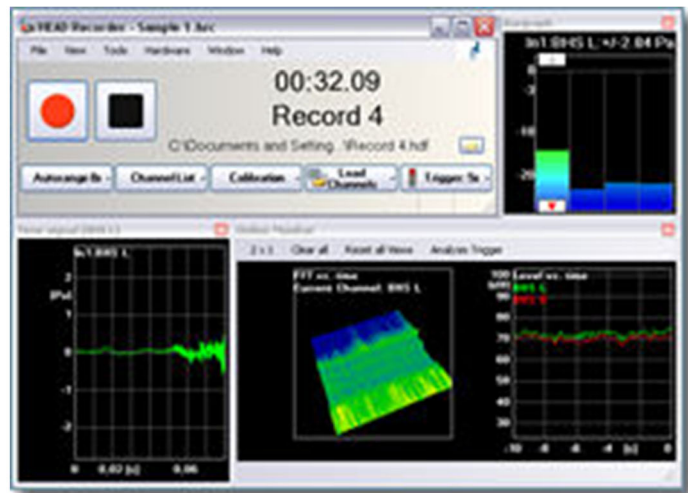
coefficients are $R^2 = 0.97$ ($D < 0$) and $R^2 = 0.99$ ($D > 0$), respectively, where D is the distance from each measuring point to center of the track.

(2) Frequency domain analysis

Figure 16 shows the 1/3 octave frequency spectrum of vibration measured in the top platform under the 4 settings. From the figures, the shapes of the frequency spectrum are very similar regardless which track the train was running on and how far the measurement point was from the center of the track.

The main vibration energy in the platform when the train is passing by the throat area is between 20 and 100 Hz. It is between 10 and 50 Hz when train is passing by the inspection area. With the increase of the distance from the center of the track, the vibration level decreases in general, though there is no obvious decrease below 10 Hz. This shows that the vibration was attenuated mainly in the middle- and high-frequency bands when transmission is inside the top platform. There is only very limited attenuation for the frequency bands below 10 Hz. This can be a potential problem, as the most sensitive frequency band of the human body given by the ISO 10137-2007 (ISO 2007) is between 4 and 8 Hz.

In order to investigate the vibration propagation characteristics at particular frequency bands, vibration levels (measured

under settings 3 and 4) are plotted against distance for a number of 1/3 octave frequency bands with the central frequencies of 2.5, 5, 25, 40, 80, and 160 Hz, in Fig. 17. The best fit of the data (using B-spline) was also shown in the figure as solid lines.

In Fig. 17, with the increase of distance to the track, (1) the levels in low-frequency bands, 2.5 and 5 Hz, are nearly the same; (2) in the middle-frequency bands, 25 and 40Hz, the levels decrease gradually; and (3) in the high-frequency bands, 80 and 160 Hz, the levels decrease much faster than the other bands.

Compared with the high-frequency bands, the middle-frequency bands have higher vibration levels and smaller attenuation rates. The human body is more sensitive to the medium- and low-frequency vibration than the high-frequency vibration. The low-frequency bands have only small vibration levels for this case. Therefore, vibration in the middle-frequency bands and relevant mitigation measures should be the particular focused during the design of over-track buildings.

Vibration transmission between floors

Table 4 shows the average vibration level measured in both floors and in the top platform. From Table 3, the vibration levels measured in the platform and the first floor

Table 3 Vibration response of vibration source in the metro depot

Position	Analysis index	Throat area		Inspection depot	
		Rail	Ballast bed	Rail	Supporting column
First floor underground	Average acceleration peak value (m/s^2)	12.78	0.51	12.73	0.61
	Main frequency band (Hz)	50~800	50~200	100~900	100~200
Second floor underground	Average acceleration peak value (m/s^2)	17.67	0.26	2.68	0.16
	Main frequency band (Hz)	50~800	50~200	100~900	100~200

Fig. 11 Acceleration time histogram of vibration source. **a** Throat area and **b** inspection area
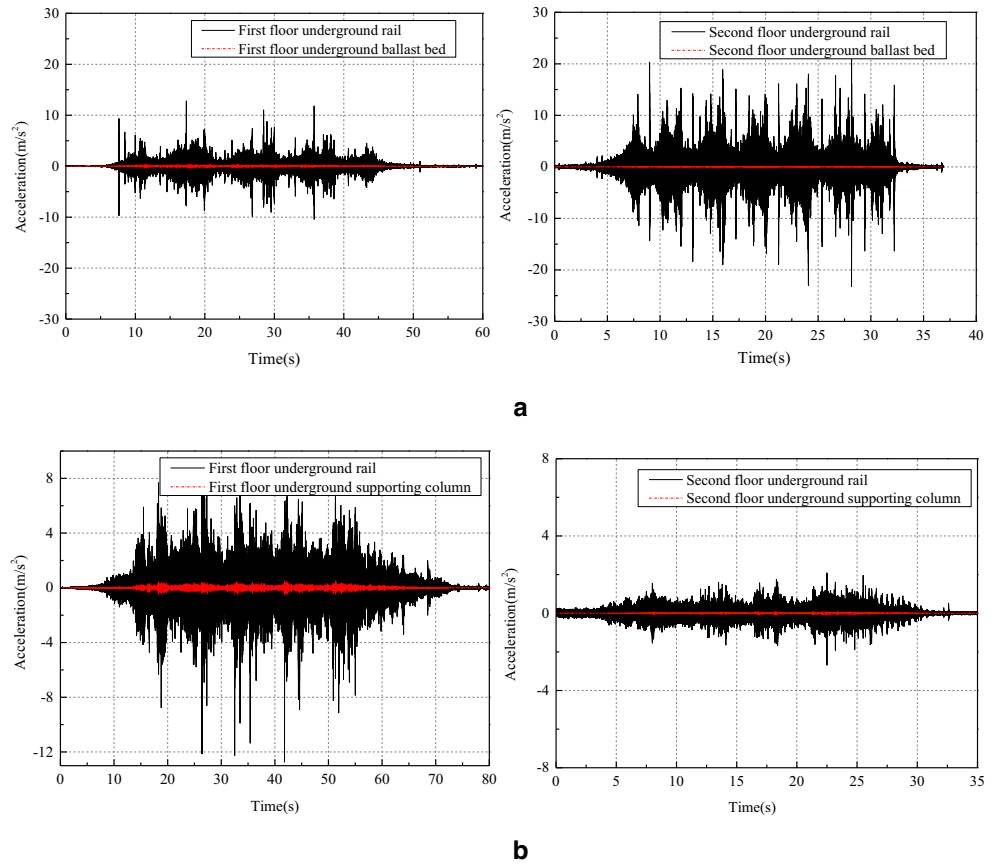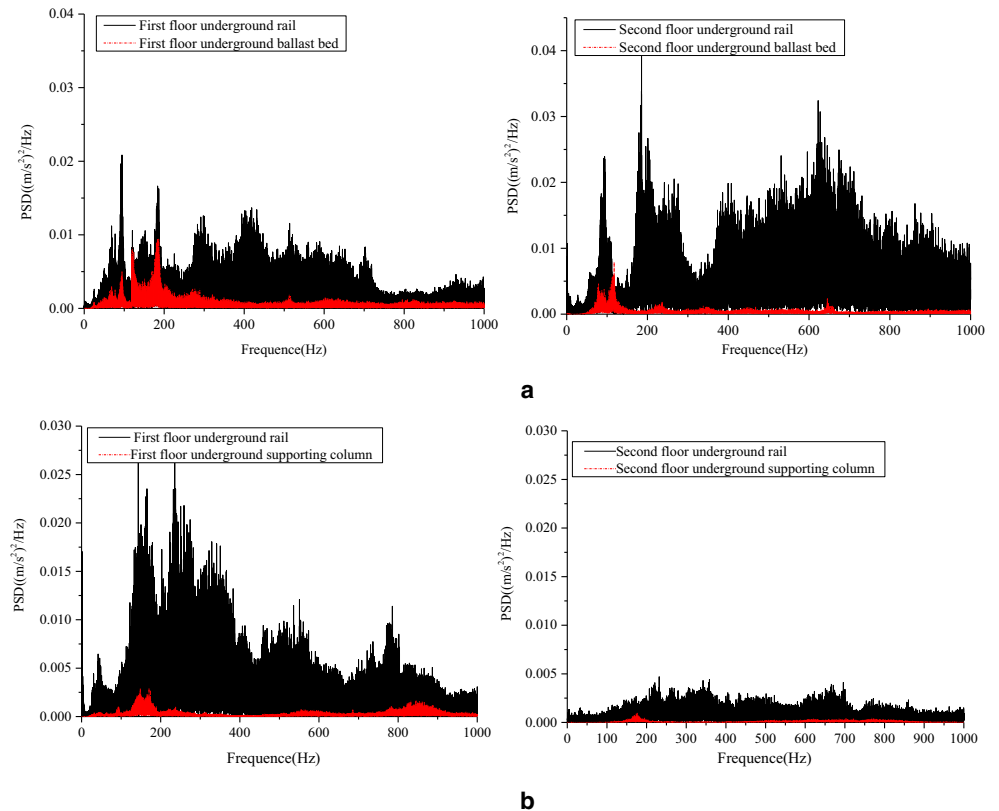

a

b

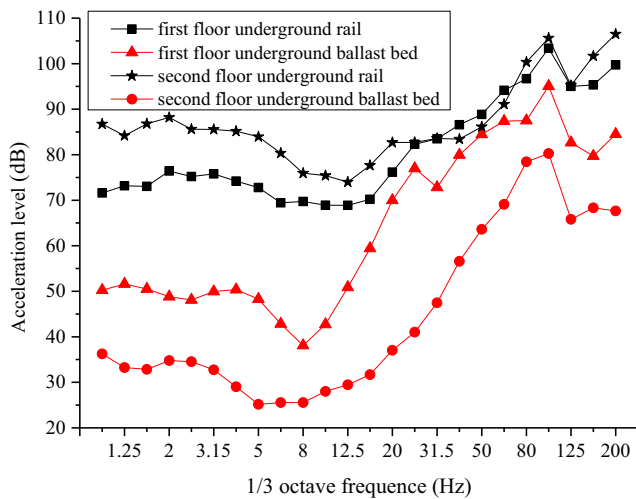Fig. 12 PSD of vibration source. **a** Throat area and **b** inspection area

a

b

Fig. 13 Rail- ballast acceleration levels in 1/3 octave bands

underground was actually 3–4 dB larger than in the second floor underground when the train was running on the second floor underground. This may be due to the fact that the measurement points were set directly on the foundation in the second floor underground and the vibration energy was partially attenuated by the surrounding soil before reaching the transducers. However, the measurement points in the first floor underground and in the top platform were set on the floor/platform panel which are linked to the rail through "rail-supporting column-foundation-structural column-platform," without soil attenuation. Besides that, the floor/platform panels have much smaller stiffness than the earth. The running train in the second floor underground may excite bending vibration in the floors above and increase the vibration level. When the train was running on the first floor underground, the averaged acceleration level measured in the first floor panel underground was 76.6 dB, and the level measured in the top platform was about 6 dB smaller.

Figure 18 shows the relevant frequency spectrum in 1/3 octave bands. From the figure, the vibration levels measured
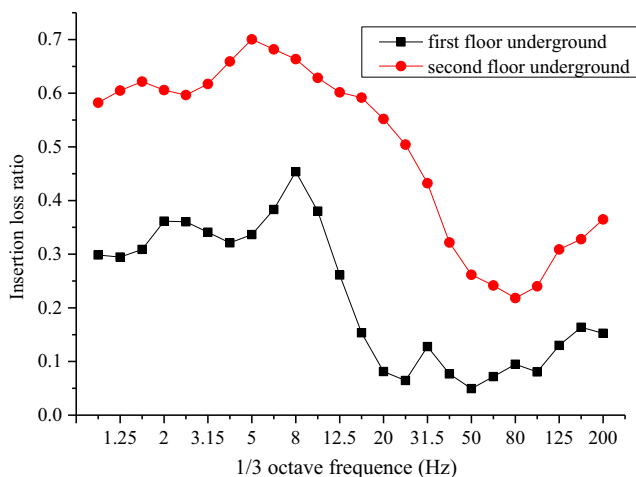

Fig. 14 Rail-ballast insertion loss ratio in 1/3 octave bands

in the first floor underground and the top platform are larger than that in the second floor underground for most of the frequency bands except those below 2 Hz, especially above 20 Hz. This agrees with the result shown in Table 3. When the train was running on the first floor underground, the vibration level in the top platform are smaller, except in the frequency bands from 6.3 to 16 Hz.

Vibration comfort level analysis

Vibration level analysis

The vibration induced by the trains entering and leaving the depots can transmit to the over-track buildings through the structures and have an impact on the residents. Unlike the railway main line where the distance from the track to the nearby building is constant, the vibration transmit from the underground depot depends on the location of the track. If the track train running on is directly under the building, the vibration level in the building can reach a very high level. However, there could be only 3–4 trains each morning/night passing directly under the building. If the track train running on is far away from the building, the vibration level can be significantly smaller depending on the distance. Therefore, using a single averaged value to assess the vibration level induced by the trains in the underground depot may not reflect the real situation reasonably. Here, the vibration level obtained from different groups is based on the area the train is running. The train pass-by events can be divided into three groups according to the area the train is passing:

> First group: The train running on the first floor underground in the same area below the measuring points
> Second group: The train running on the first floor underground in the other area
> Third group: The train running on the second floor underground

Figure 19a shows the vibration level measured at throat area, where C1 is directly above the turnout and C4, C5, C6, and C7 are above the non-turnout area. Figure 19b shows the vibration levels measured at inspection area. The averaged level calculated in the first group situation was much higher than the other two groups. The vibration levels obtained in the other two groups were about 10–20 dB smaller. The averaged levels measured in the top platform directly above the turnout and non-turnout areas in the throat area are 78.5 and 73.9 dB, respectively. This indicated that the vibration induced by the train passing through the turnout area is much larger than that in the non-turnout area, which is 4.6 dB larger in this case. The test results also show big difference depending on the location of the track and the location of the measuring point, even within the same area. When the train were running from the

Fig. 15 Acceleration vibration level fitting-error bar chart area under different settings. **a** Setting 1, **b** setting 2, **c** setting 3, **d** setting 4
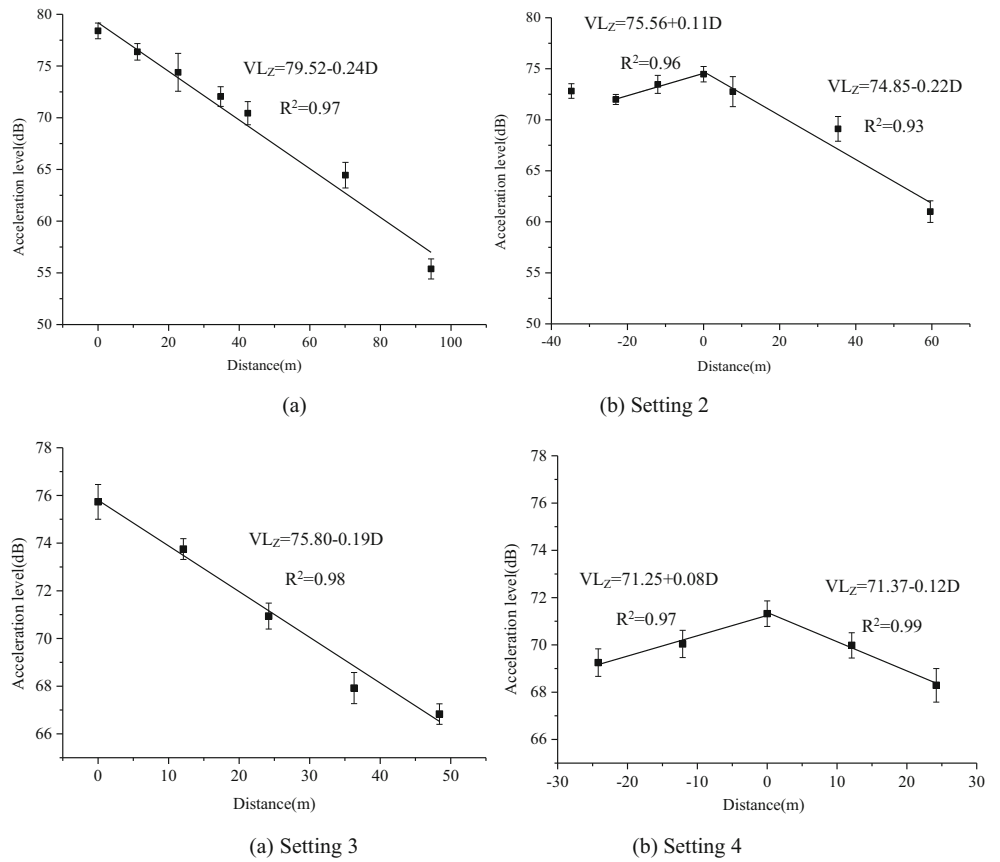

(a)

(b) Setting 2

(a) Setting 3

(b) Setting 4

Fig. 16 Vertical 1/3 octave frequency spectrum of top platform under different settings. **a** Setting 1, **b** setting 2, **c** setting 3, **d** setting 4
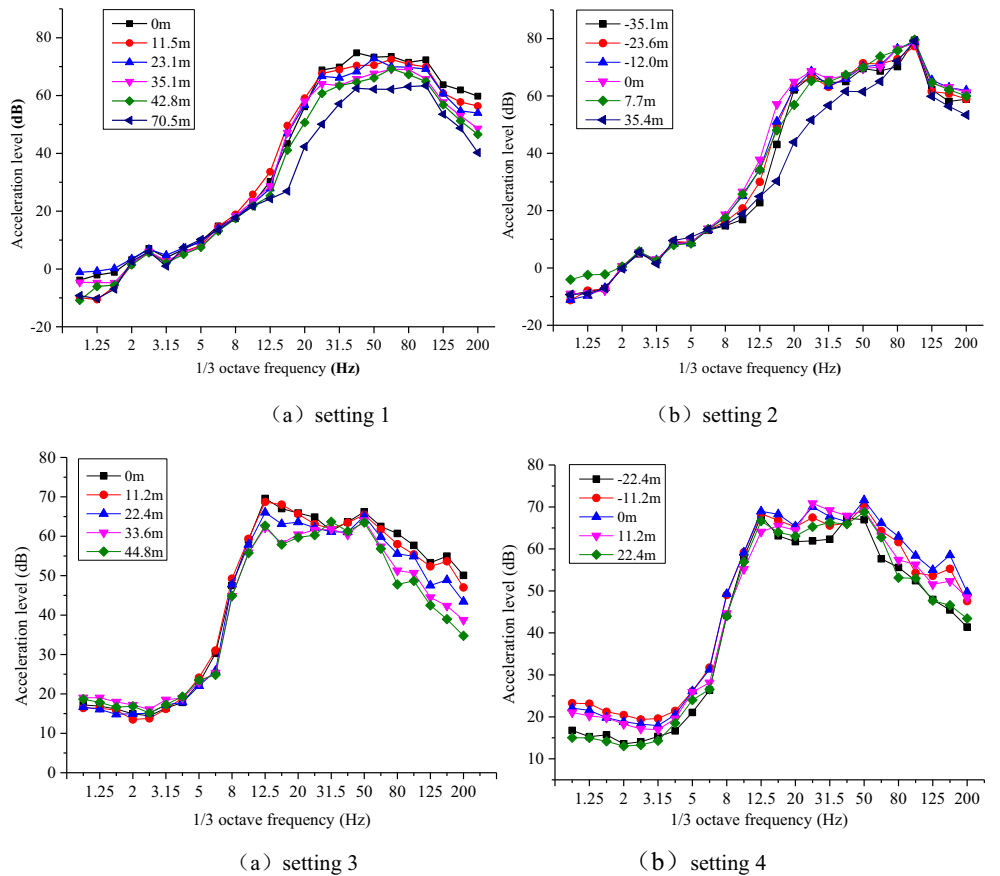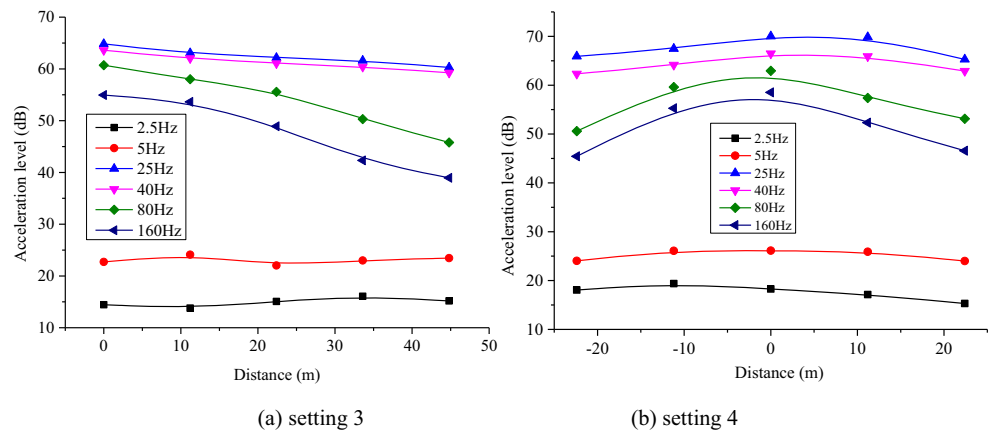

（a）setting 1

（b）setting 2

（a）setting 3

（b）setting 4

Fig. 17 Relationship between each frequency vibration levels and distances under different settings. **a** Setting 3 and **b** setting 4

(a) setting 3   (b) setting 4

turnout directly below the measuring points, the vibration level was 81 dB, while the level reduced to 74 dB when the trains moved 3 track spacing away from it. The vibration response of the platform induced by the train running in throat area is larger than that induced by the train running in the inspection area, and the difference between them can reach 5~10 dB. The vibration in the top platform induced by the train running on the first floor underground is much larger than the train running on the second floor underground; it may be due to exciting the vibration mode of the structure when the trains are running on the first floor underground.

Vibration comfort level evaluation

According to the Chinese standard GB10071, at least 20 trains should be recorded continuously, and an averaged value should be used for the vibration level evaluation. However, from the results shown in the previous sections, the vibration from the underground depot can vary significantly depending on the location of the track train running on. Therefore, vibration levels obtained from three different scheme were used here, considering the relationship between the working track and the measuring location, as shown in Fig. 20.

The first evaluation scheme is considered averaged value of the vibration level measured directly above the passing train. The second evaluation scheme took the averaged value of the vibration level when the trains were running on different tracks at the same group area. This value excluded the impacts from the trains running on the second floor underground.

Since the depot was divided into the east and west areas structurally, only the east area was considered here. The third evaluation scheme took the averaged value of all the measurements. Results are shown in Table 5.

From Table 5, the following can be drawn:

(1) The results of scheme 1 were larger than other schemes, with 81 dB in the top platform over the throat turnout area, 75.7 dB in the top platform over the throat non-turnout area, and 70.4 dB in the top platform over the inspection area.
(2) From the results of scheme 2, the vibration level in the top platform over the throat turnout area is 78.5 dB, 6.5dB larger than the limit. The vibration level in the top platform over the throat non-turnout area is 73.9 dB, 1.9 dB larger than the limit. And the vibration level in the top platform over the train inspection area is 68.5 dB, within the given limit.
(3) The result from scheme 3 is smaller than the other two, because the vibration in the platform caused by the train running on the second floor underground is much smaller than the others. Therefore, it resulted a smaller averaged vibration level.
(4) For the underground metro depot, the track distribution area is large, and there are only several train pass-by events under a certain measuring point every day, so the result of scheme 1 is obtained from the several train pass-by events every day. Scheme 3 considers all train pass-by events, and the vibration of the platform is

Table 4 Average vibration level of each floor at inspection area (dB)

Settings	Index	Second floor underground	First floor underground	Platform
Train running at second floor underground	Vibration acceleration level	54.0	57.6	57.96
	Attenuation value	—	3.6	3.96
Train running at first floor underground	Vibration acceleration level	—	76.6	70.4
	Attenuation value	—	—	−6.2

Fig. 18 1/3 octave frequency spectrum of floor slabs vibration acceleration. **a** Train running in the second floor underground and **b** train running in the first floor underground

(a) Train running in the second floor underground

(b) Train running in the first floor underground
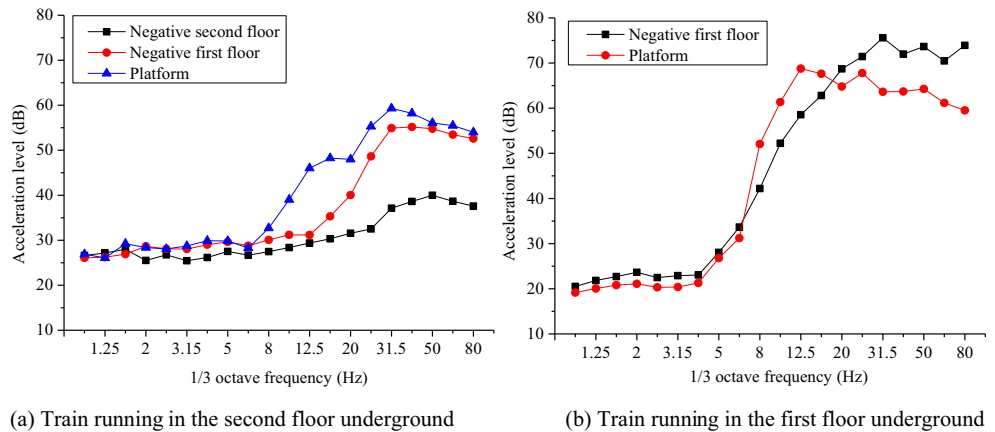
induced by the trains running in the west area, and the underground second floor is very small, even the human body cannot perceive it. The result of scheme 2 is obtained from the trains passing through the same group area, which is more suitable for evaluating the vibration comfort level of such structure. Therefore, we suggest that scheme 2 should be used to evaluate the vibration level of such structure.

Conclusion

In this paper, experimental campaigns were conducted in the largest underground multiple-story metro depot in Asia, and the characteristics of train-induced vibration in a new structure of metro depot were studied. Both the time and frequency domain methods were employed for data analysis. The following conclusions can be drawn:

(1) The train floor structure interaction leads to the maximum acceleration of the vibration source in the first floor underground larger than that in the second floor

underground. The maximum acceleration of ballast bed at the throat area on the first and second floors underground are about 0.51 and 0.26m/s^2, respectively, and the main frequency components are between 50 and 200 Hz. The natural frequency of the over-track building floor slab should avoid the main frequency components in the future design.

(2) The vibration in the top platform decreases linearly with the distance from the center line of the track. When the trains are running on the track at the edge area, the linear attenuation rate is about 0.2 dB/m. If the over-track buildings are constructed above the throat platform within 30 m from the track, the vibration level should be carefully investigated, and relevant mitigation measures may need to be considered.

(3) The mid- and low-frequency vibrations, which the human body is more sensitive to, are attenuated slower than the high-frequency vibration. Therefore, mitigation measures for mid–low-frequency vibration should be the focus more in the design of future underground metro depots.

(4) It is easy to excite the vibration mode of the structure when the trains are running on the first floor

Fig. 19 Acceleration vibration level of platform. **a** Throat area and **b** inspection area
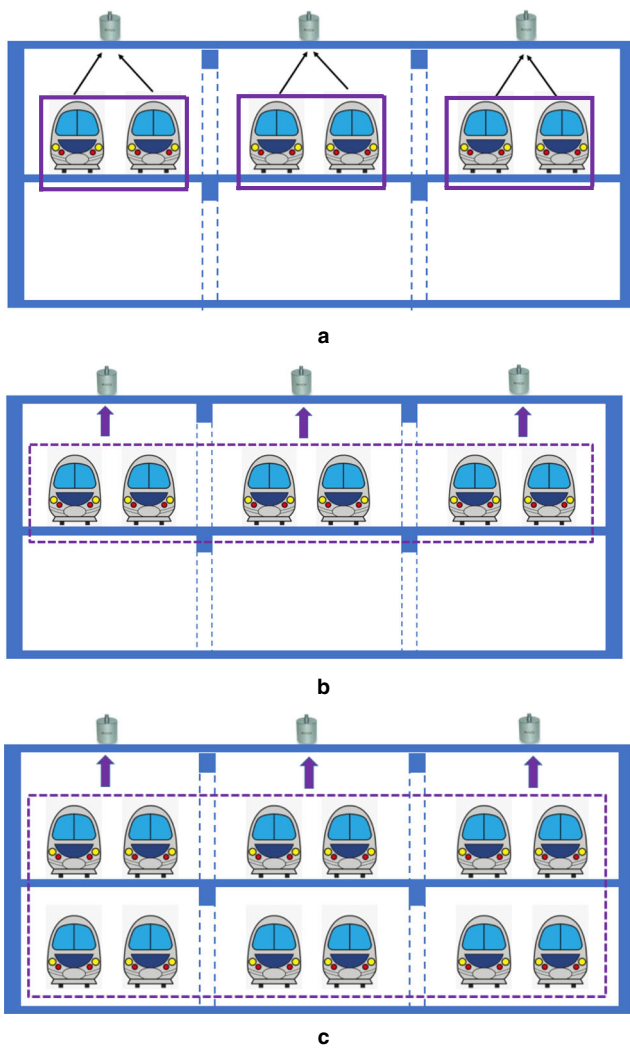

(a) throat area

(b) inspection area
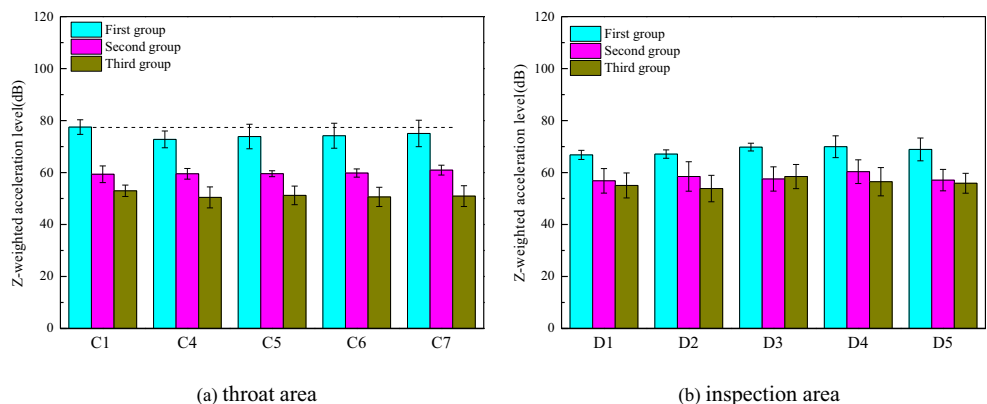
Fig. 20 Three different evaluation schemes. **a** Evaluation scheme 1 (downward running), **b** Evaluation scheme 2 (running on first floor underground in the same group area), and **c** evaluation scheme 3 (all running trains)

structural dynamic behavior of the over-track buildings induced by the train running on the floor slab underground should be the focus.

(5) The throat area has many rail joints and turnouts which can lead to a larger vibration level in the train pass-by events. From the measurement obtained in this study, the level exceeded the limit given for human vibration comfort. Mitigation measures should be carefully considered in the area.

Declaration

underground, so the vibration in the top platform induced by the train running on the first floor underground is much larger than train running on the second floor underground. Therefore, in the future design, if the underground metro depot has more than one floor, the

Table 5 Vibration level under different evaluation schemes (dB)

Region	Evaluation scheme 1	Evaluation scheme 2	Evaluation scheme 3	Limit value
Platform of throat turnout area	81.0	78.5	65.63	72
Platform of throat non-turnout area	75.7	73.9	64.51	
Platform of inspection area	70.4	68.5	61.05	

References

Aires C, Alves CP, Paulo AM et al (2017) Prediction of vibrations and radiated noise due to railway traffic: a comprehensive hybrid model based on a finite element method and method of fundamental solutions approach[J]. J Vib Acoust 139(6):061009 1-10. https://doi.org/10.1115/1.4036929

Cao ZL, Guo T (2018) Measurement and analysis of vibrations in a residential building constructed on an elevated metro depot [J]. Measurement 125:394–405. https://doi.org/10.1016/j.measurement.2018.05.010

China Association of Metros (2021) Overview of urban rail transit lines in mainland China in 2020. https://www.camet.org.cn/xxfb/7270

Connolly DP, Kouroussis G, Woodward PK, Alves Costa P, Verlinden O, Forde MC (2014) Field testing and analysis of high speed rail vibrations[J]. Soil Dyn Earthq Eng 67:102–118. https://doi.org/10.1016/j.soildyn.2014.08.013

Coulier P, Lombaert G, Degrande G (2014) The influence of source-receiver interaction on the numerical prediction of railway induced vibrations[J]. J Sound Vib 333:2520–2538. https://doi.org/10.1016/j.jsv.2014.01.017

Federal Transit Administration (US) (2006) Transit noise and vibration impact assessment. The Administration, Washington

Galvín P, Domínguez J (2009) Experimental and numerical analyses of vibrations induced by high-speed trains on the Córdoba-Málaga line [J]. Soil Dyn Earthq Eng 29(4):641–657. https://doi.org/10.1016/j.soildyn.2008.07.001

GB10070-88 (1988) Standard of vibration in urban area environment. China's State Environmental Protection Administration

Guo T, Cao Z, Zhang Z, Li A (2017) Numerical simulation of floor vibrations of a metro depot under moving subway trains [J]. J Vib Control 24(18):4353–4366. https://doi.org/10.1177/1077546317724322

He W (2018) Vertical dynamics of a single-span beam subjected to moving mass-suspended payload system with variable speeds [J]. J Sound Vib 418:36–54. https://doi.org/10.1016/j.jsv.2017.12.030

He W (2019) Field measurement and evaluation of noise and vibrations induced by bridge cranes in full-scale over-track buildings [J]. Environ Sci Pollut Res 26:36515–36537. https://doi.org/10.1007/s11356-019-06759-7

He W, Zou C, Pang Y, Wang X (2020) Environmental noise and vibration characteristics of rubber-spring floating slab track [J]. Environ Sci Pollut Res, online publication 28:13671–13689. https://doi.org/10.1007/s11356-020-11627-w

Hussein M, Hunt H (2015) The use of sub-modelling technique to calculate vibration in buildings from underground railways [J]. P I Mech Eng F-J Rai 229(3):303–314. https://doi.org/10.1177/0954409713511449

International Organization for Standardization (2007) ISO10137: Bases for design of structure-serviceability of buildings and walkways against vibrations

Ju SH (2007) Finite element analysis of structure-borne vibration from high-speed train [J]. Soil Dyn Earthq Eng 27(3):259–273. https://doi.org/10.1016/j.soildyn.2006.06.006

Kouroussis G, Verlinden O, Conti C (2011a) Free field vibrations caused by high-speed lines: measurement and time domain simulation [J]. Soil Dyn Earthq Eng 31(4):692–707. https://doi.org/10.1016/j.soildyn.2010.11.012

Kouroussis G, Verlinden O, Conti C (2011b) Efficiency of resilient wheels on the alleviation of railway ground vibrations[J]. P I Mech Eng F-J Rai 226(4):381–396. https://doi.org/10.1177/0954409711429210

Kouroussis G, Conti C, Verlinden O (2013) Experimental study of ground vibrations induced by Brussels IC/IR trains in their neighborhood [J]. Mech Ind 14(2):99–105. https://doi.org/10.1051/meca/2013059

Kouroussis G, Connolly DP, Vogiatzis K, Verlinden O (2015) Modelling the environmental effects of railway vibrations from different types of rolling stock: a numerical study [J]. Shock Vib 2015:1–15. https://doi.org/10.1155/2015/142807

Lopes P, Costa PA (2014) Influence of soil stiffness on building vibrations due to railway traffic in tunnels: numerical study [J]. Comput Geotech 61(3):277–291. https://doi.org/10.1016/j.compgeo.2014.06.005

López-Mendoza D, Romero A (2017) Scoping assessment of building vibration induced by railway traffic [J]. Soil Dyn Earthq Eng 93:147–161. https://doi.org/10.1016/j.soildyn.2016.12.008

Ma M, Xu LH, Du LL et al (2020) Prediction of building vibration induced by metro trains running in a curved tunnel [J]. J Vib Control, online publication 27:515–528. https://doi.org/10.1177/1077546320930910

Metrikine AV, Vrouwenvelder ACWM (2000) Surface ground vibration due to a moving train in a tunnel: two-dimensional model [J]. J Sound Vib 234(1):43–66. https://doi.org/10.1006/jsvi.1999.2853

National Development and Reform Commission (2019) Reply on the fourth phase construction plan of Chengdu urban rail transit (2019-2024). (in Chinese) https://www.ndrc.gov.cn/xxgk/zcfb/ghwb/201908/t20190821_962257.html

Persson P, Persson K (2016) Numerical study on reducing building vibrations by foundation improvement [J]. Eng Struct 124:361–375. https://doi.org/10.1016/j.engstruct.2016.06.020

Sanayei M, Maurya P, Moore JA (2013) Experiment of building foundation and ground-borne vibrations due to surface trains and subways [J]. Eng Struct 53:102–111. https://doi.org/10.1016/j.engstruct.2013.03.038

Sanayei M, Anish KP, Moore JA, Brett CR (2014) Measurement and prediction of train-induced vibrations in a full-scale building [J]. Eng Struct 77:119–128. https://doi.org/10.1016/j.engstruct.2014.07.033

Tao ZY, Wang Y, Sanayei M, Moore JA, Zou C (2019a) Experimental study of train-induced vibration in over-track buildings in a metro depot [J]. Eng Struct 198:109473. https://doi.org/10.1016/j.engstruct.2019.109473

Tao ZY, Wang YM, Zou C, Li Q, Luo Y (2019b) Assessment of ventilation noise impact from metro depot with over-track platform structure on workers and nearby inhabitants [J]. Environ Sci Pollut Res 26(9):9203–9218. https://doi.org/10.1007/s11356-019-04378-w

Vogiatzis K, Mouzakis H (2018) Ground-borne noise and vibration transmitted from subway networks to multi-storey reinforced concrete buildings [J]. Transport 33(11):1–8. https://doi.org/10.3846/16484142.2017.1347895

Xie WP, Zhao N, He W et al (2013) Analysis on vibration serviceability of over-track buildings [J]. Chin Civil Eng J 46(06):90–96. (in Chinese). https://doi.org/10.15951/j.tmgcxb.2013.06.017

Zou C, Wang YM, Wang P, Guol J (2015) Measurement of ground and nearby building vibration and noise induced by trains in a metro depot [J]. Sci Total Environ 536:761–773. https://doi.org/10.1016/j.scitotenv.2015.07.123

Zou C, Wang Y, Moore JA, Sanayei M (2017) Train-induced field vibration measurement of ground and over-track buildings [J]. Sci Total Environ 575:1339–1351. https://doi.org/10.1016/j.scitotenv.2016.09.216

Zou C, Moore JA, Sanayei M, Wang Y (2018) Impedance model for estimating train induced building vibrations [J]. Eng Struct 172:739–750. https://doi.org/10.1016/j.engstruct.2018.06.032

Zou C, Moore JA, Sanayei M, Wang Y, Tao Z (2020) Efficient impedance model for the estimation of train-induced vibrations in over-track buildings [J]. J Vib Control, online publication 27:924–942. https://doi.org/10.1177/1077546320935285